UDK 622.031.2:543.456
Original scientific article/Izvirni znanstveni članek

ISSN 1580-2949
Mater. Tehnol.

APPLICATION OF ATOMIC FORCE MICROSCOPY IN PREPARING Ni-Al LAYER USING A TWO-STAGE PROCESS

UPORABA MIKROSKOPIJE NA ATOMSKO SILO ZA PRIPRAVO Ni-Al TANKIH PLASTI Z DVOSTOPENJSKIM POSTOPKOM

Ningning Li[1,2,3], Zhenjie Hao[1,2], Lei Xu[1,2,*], Xi Chen[1,2], Jin Peng[1,2], Leyu Wei[1,2], Mingqi Tang[1,2], Yuping Tong[1,2], Zicheng Ling[1,2], Yimin Li[3]

[1]School of Materials Science and Engineering, North China University of Water Resources and Electric Power, Zhengzhou 450045
[2]Henan Engineering Research Center on Special Materials and Applications of Water Conservancy and Hydropower Engineering, Zhengzhou 450045, China
[3]Luoyang Aijia Mold Manufacturing Co., Ltd, Luoyang 471000

Prejem rokopisa – received: 2024-12-09; sprejem za objavo – accepted for publication: 2025-02-17

doi:10.17222/mit.2024.1352

A Ni-Al layer can provide substrate properties and has received widespread attention. This study investigates the morphology and composition of a Ni-Al layer fabricated on a steel substrate using a two-step method. Initially, an internal nickel layer was deposited via electroplating, followed by an aluminization process. The morphological and compositional characteristics of the resulting Ni-Al layer were analyzed using metallographic microscopy, scanning electron microscopy (SEM) coupled with energy-dispersive spectroscopy (EDS), and atomic force microscopy (AFM). The results revealed that the morphological changes to the Ni-Al layer are influenced by the aluminum content in the infiltration agent, and the data from AFM confirm this.

Keywords: Ni-Al layer, atomic force microscopy, nickel layer, morphology

Tanka Ni-Al plast lahko ima posebne lastnosti in zato med raziskovalci vzbuja veliko pozoornosti. V tem članku avtorji opisujejo študijo morfologije in sestave Ni-Al plasti izdelanih na jekleni podlagi z uporabo dvostopenjske metode. Najprej so avtorji nanesli tanko plast Ni s postopkom elektroplatiranja, kateremu je sledil postopek aluminiziranja. Avtorji so nato morfološko in mikrokemijsko analizirali izdelane Ni-Al plasti s pomočjo metalografskega in vrstičnega elektronskega mikroskopa (SEM) s prigrajenim spektroskopom na osnovi energije despergiranih elektronov (EDS). Karakterizacijo Al-Ni plasti so izvedli še z mikroskopom na atomsko silo (AFM; angl.: Atomic Force Microscopy). Rezultati raziskav so pokazali, da so morfološke in fazne spremembe Ni-Al plasti odvisne od vsebnosti Al v infiltracijskem sredstvu. To so potrdili tudi rezultati karakterizacije z AFM.

Ključne besede: tanke plasti na osnovi Ni-Al, mikroskopija na atomsko silo, plast niklja, morfologija

1 INTRODUCTION

Powder aluminizing is a commonly used surface treatment.[1,2] It cannot only improve the high-temperature oxidation resistance of the substrate, it can also increase the corrosion resistance in a number of acids, alkalis, or other sulfur-containing media, and it can also improve the wear resistance of materials.[3–5] Therefore, it is widely used in the petroleum, chemical, metallurgy, transportation and other industries. The microstructure of the aluminization layer is influenced by several key factors, including the composition of the cementation agent, the temperature and duration of the infiltration process, as well as the specific type of substrate employed.[5]

In recent years, a series of intermetallic compound coatings have been researched due to their high melting points, low densities, and excellent corrosion resistance at high temperatures. Ni-Al intermetallic compound coatings have been applied to high-temperature alloy surfaces, because it is easy to form a dense alumina layer at high temperatures.[6,7] To make nickel-aluminium coatings on other metal surfaces, a two-step process of nickel plating and powder aluminizing has been invented.[8–10] A. Bogdanov et al.[10] studied the Ni_2Al_3/Ni layered coating during isothermal oxidation and found that earlier stages of the coating oxidation result in the formation of separate alumina areas-plate-like crystals agglomerates, which increase in size with increasing exposure time and grow together into a continuous alumina scale layer. This method not only has the advantage of good quality, simple operation, small technical difficulty, and less investment in equipment, but also weakens the influence of the chemical composition of the substrate on forming aluminized coating, and a low aluminized temperature can be used. The low temperature can also protect the substrate properties, so it has been researched recently.

There are many aluminizing methods and it is a mature technology. The three main methods include pack aluminizing, hot-dip aluminizing, and thermal spraying.[11–13] These methods have their process characteristics, and the formation and structure of aluminide layers are also varied. For example, the aluminized surface is

*Corresponding author's e-mail:
xulei2022@ncwu.edu.cn (Lei Xu)

porous after heat treatment of aluminium impregnation, which leads to a higher rejection rate and a brittle layer that is easy to peel off. Pack aluminizing has been widely used, due to the matrix being surrounded by infiltration agents, resulting in less leakage and the easy acquisition of a dense layer, and the device is simple and easy to operate additionally.[14]

Among the influencing factors of pack aluminizing, the aluminized temperature and pack Al content are the main factors affecting the coating formation, while the aluminized time only affects the coating thickness.[15,16] But the high aluminized temperature can degrade the creep resistance of the steels.[17] Therefore, the low-temperature pack aluminizing is more popular.[18,19]

AFM is an analytical instrument used to study the surface structure of solid materials, including insulators. The basic principle is to fix one end of a microcantilever that is extremely sensitive to weak forces, and the other end has a tiny needle tip. There is an extremely weak repulsive force between the tip atoms and the surface atoms of the sample. By using optical testing or tunneling-current detection methods, the surface-morphology information can be obtained by measuring the distance change between the needle tip and the sample. The main application areas of atomic force microscopy are very wide, and they can be applied to various fields such as biology, materials science, the semiconductor industry, etc.

In our preliminary study, a nickel electroplating process was initially employed to deposit a nickel layer onto the steel substrate. Subsequently, four distinct Ni-Al layers were fabricated using cementation agents with varying aluminum contents. The aluminization process was conducted at 650 °C, a temperature below the melting point of aluminum, as detailed in our previously published work.[20] In the current investigation, the cross-sectional and surface morphology of the Ni-Al layers were comprehensively characterized using metallurgical microscopy and SEM coupled with EDS. Furthermore, AFM was utilized to analyze the two-dimensional and three-dimensional surface topography of the layers, providing enhanced resolution for morphological observation.

2 EXPERIMENTAL PART

2.1 Materials

Ordinary Q235 steel was selected as the substrate, with dimensions of (10 × 10 × 2) mm, and the nominal chemical composition was shown in **Table 1**. Detailed experimental procedures of nickel plating and pack aluminizing used were described in our previous work and the main conclusions were already analyzed and discussed.[20] For a better understanding, the experimental process is repeatedly described as the following.

Before plating, the substrate was mechanically flattened with 120, 240, 320, 400, 600 and 800 metallographic papers, polished and ultrasonically cleaned with acetone for 5 min, then washed with distilled water and activated in 5 *w*/% HCl for 20 s. Finally, it was washed with distilled water again and quickly immersed into a bath. The electroplating power supply was a DC power supply. To maintain the uniformity of solution, mechanical stirring with a magnetic stirrer located at the container bottom was used. Four nickel-plated samples were prepared. The samples were washed with distilled water and ethanol repeatedly, being removed from the cell. The pack cement is composed of the Al powder, $AlCl_3$, and Al_2O_3 powder as the filler. A series of samples were manufactured, and the contents of the Al power were (8, 15, 50 and 70) *w*/%. The activating $AlCl_3$ content was 5 *w*/%, and the Al_2O_3 reminder was the inert filler. The substrate was embedded in a packed mixture in an alumina crucible and then positioned in a vacuum tube furnace with argon. After placing the crucible, the tube furnace was filled with argon gas three times to clean and exhaust the oxygen, and then start the set heating program. The furnace was heated at a rate of 10 °C/min and the dwell time was 20 h at a temperature of 650 °C. Eventually, the samples were removed after having been cooled to room temperature, and alcohol was used to remove the adhered particles. The preliminary main outcomes were summarized as follows: the layer phase was mainly composed of $NiAl_3$ and Ni_2Al_3.[20]

2.2 Surface characterization

The cross-sectional morphology of the layer was observed through the metallographic microscope (Olympus, CKX53, Japan). The surface morphology was characterized with a scanning electron microscope (SEM, S-3400II, Hitachi, Japan), equipped with the energy dispersive spectrometer (EDS). In addition, the two-dimensional and three-dimensional morphology characteristics of the Ni-Al layer were also obtained through atomic force microscopy (AFM, Multimode 8, United States).

3 RESULTS AND DISCUSSION

3.1 Metallographic photographs of Ni-Al layer cross-section morphology

The cross-sectional morphology of the Ni-Al layer is shown in **Figure 1**. It can be seen that the thickness of

Table 1: Nominal chemical composition of Q235 low-carbon steel (*w*/%)

Composition	C	Mn	Si	S	P	Fe
Content	0.140-0.220	0.300-0.650	0.300	≤0.050	0.045	Bal.

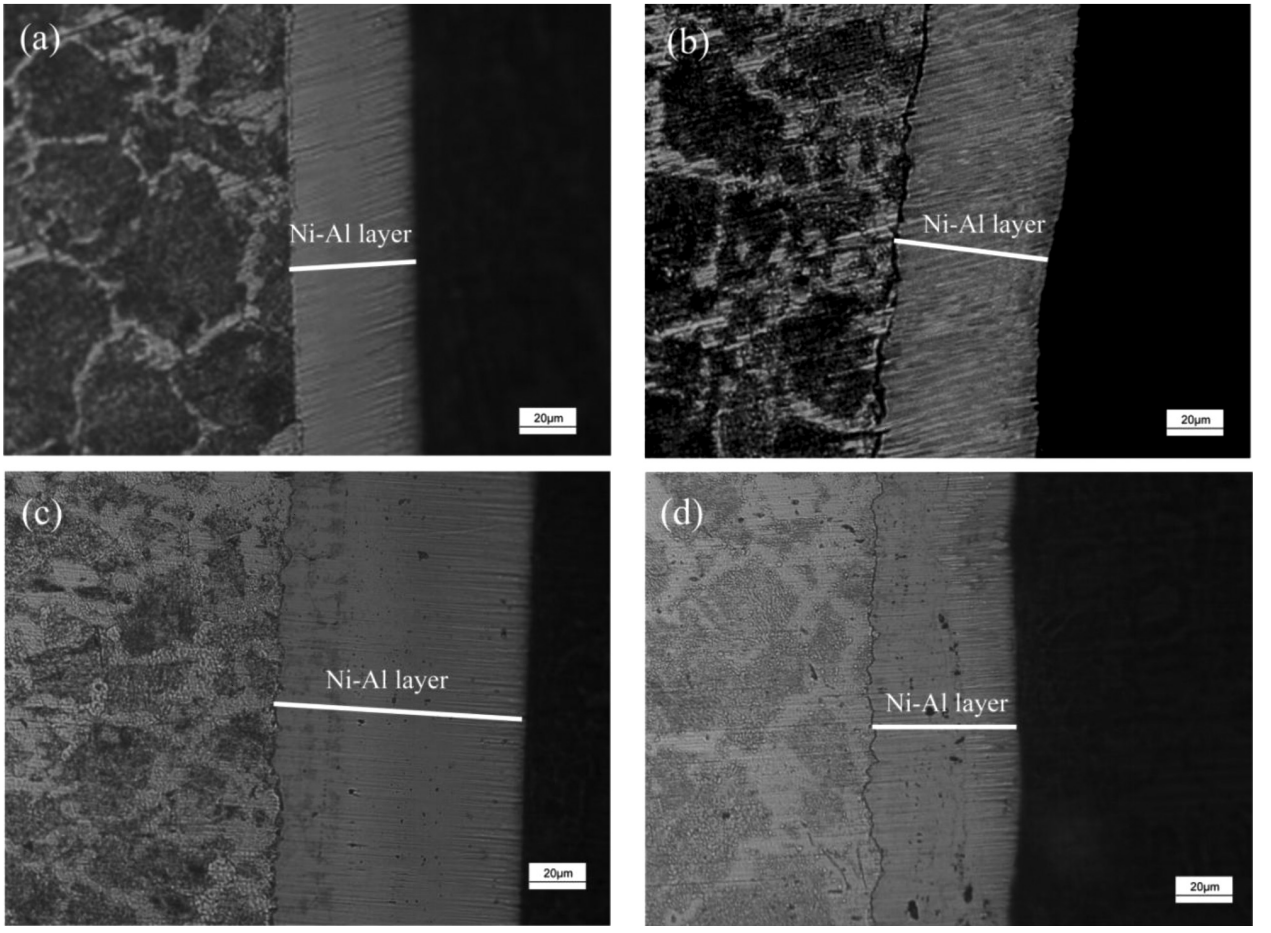

Figure 1: Metallographic photographs of Ni-Al layer cross-section fabricated with different aluminum content in the cement: a) 8 *w*/%; b) 15 *w*/%; c) 50 *w*/%; d) 70 *w*/%

the infiltration layer increases with the aluminum content in the cement increases, even at the same pack aluminizing temperature and time, as shown in **Figures 1a** to **1c**. Similar studies, such as Z. D. Xiang et al. confirm this.[21] From the cross-sectional morphology it can also be seen that a diffusion zone is formed at the interface between the Ni-Al layer and the substrate, to achieve metallurgical bonding. When the aluminum content in the cement is high, pores appear in the cross morphology, which is speculated to be related to the atomic diffusion.

It is worth noting that the layer thickness has not been continuously increasing, the thickness of the Ni-Al layer prepared with aluminum content of 70 *w*/% has decreased, which can be observed in **Figure 1 d**. Perhaps it is because, after the Ni-Al layer thickness reaches a certain level, due to the dense surface, the distance for aluminum atoms to diffuse into the interior becomes longer, the diffusion resistance and the diffusion time are also longer, so the diffusion rate slows down. At the same time, a large amount of aluminum powder accumulates on the substrate surface, which also hinders the growth of the layer to a certain extent.

3.2 SEM morphology and EDS composition of Ni-Al layer

Besides the metallographic morphology, the surface morphology of the Ni-Al layer was also observed by SEM and EDS, as shown in **Figure 2**. The Ni-Al layer prepared with 8 *w*/% aluminum content shown in **Figure 2a** has a relatively smooth surface, while the layer prepared with 15 *w*/% Al content, has an uneven surface with high and low levels, that can be seen in **Figure 2b**. The layer surface, while fabricated with 50 *w*/% Al, becomes flat again, but as the Al content continues to increase, it becomes rough again, which observed in **Figures 2c** and **2d**.

In addition to inspecting the surface Ni-Al layer morphology, the composition was also conducted using EDS, with the atomic and weight percentages presented in **Table 2**. It can be seen that in the Ni-Al layer prepared with 8 *w*/% aluminum content in the cement, the surface Ni to Al atomic percentage is close to 1.5, indicating the formation of the Ni_2Al_3 phase, which is consistent with XRD phase detection.[20] Fe appeared on the surface of the Ni-Al layer fabricated with 8 *w*/% and15 *w*/% Al in the cement, but it was not detected in the Ni-Al layer fabricated with 50 *w*/% and 70 *w*/%, due to the layer being

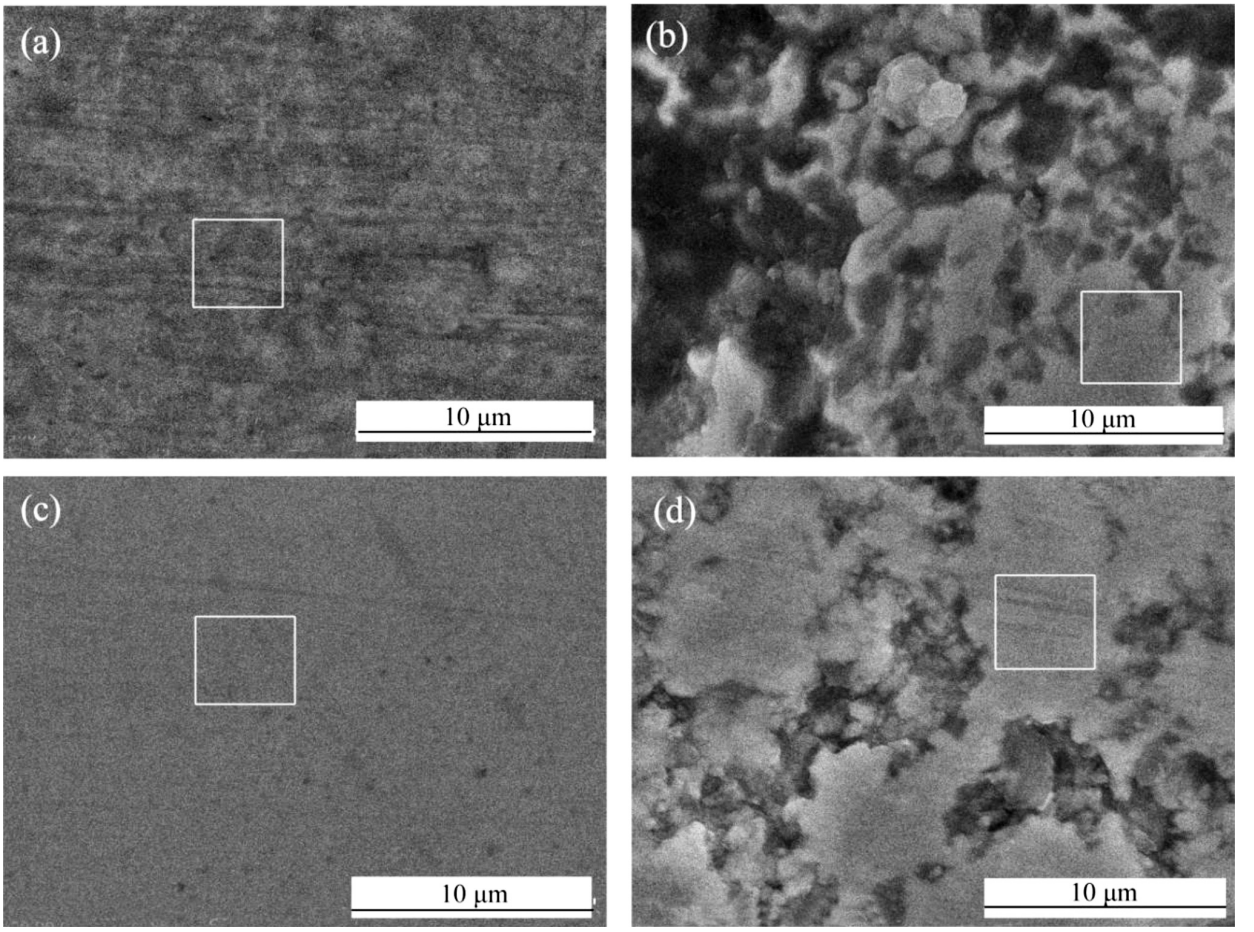

Figure 2: SEM morphology of Ni-Al layer fabricated with different Al content in the cement: 8 *w*/%; b) 15 *w*/%; c) 50 *w*/%:, d) 70 *w*/%

Table 2: Atomic and weight percentages of Ni-Al layer fabricated with different Al content in the cement:

Type	Component	8 *w*/% Al content	15 *w*/% Al content	50 *w*/% Al content	70 *w*/% Al content
Atomic percentage	Al	58.57	64.78	73.93	74.96
	Fe	0.44	11.94	0	0
	Ni	40.99	23.28	26.07	25.04
Weight percentage	Al	39.39	46.23	56.59	57.91
	Fe	0.61	17.63	0	0
	Ni	60.00	36.14	43.41	42.09

relatively thick. A curve according to **Table 2** is shown in **Figure 3**. It can be inferred that the changing trend of aluminum on the Ni-Al layer surface, indicating the aluminum-rich phase gradually formed.

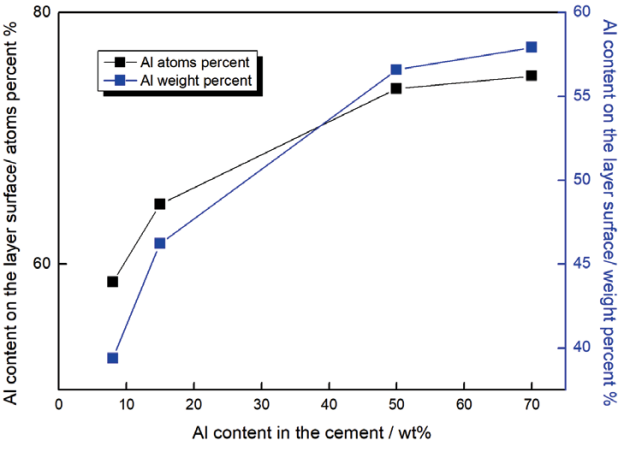

Figure 3: Atomic and weight percentages of surface components of different Ni-Al layer

3.3 Two- and three-dimensional morphology characteristics of Ni-Al layer by AFM

Atomic force microscopy (AFM) can provide true three-dimensional surface images. At the same time, AFM does not require any special sample treatment, which effectively protects the substrate.[22] **Figure 4** presents the AFM morphology of Ni-Al layers prepared under different conditions, with a scanning range of 10 μm × 10 μm, including 2D and 3D graphics, and detailed data. The color depth indicates changes in the roughness

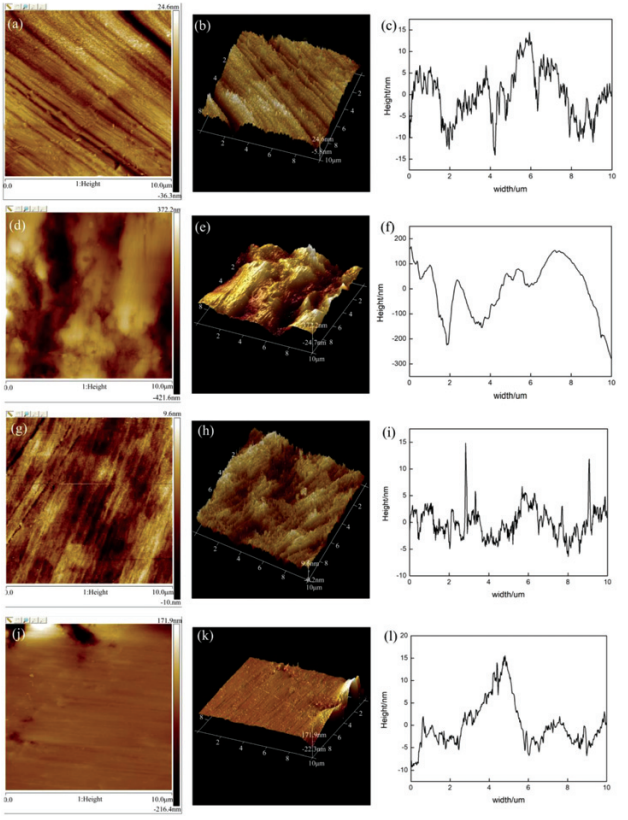

Figure 4: AFM topographies of Ni-Al layer fabricated with different Al content in the cement: a), b) and c): 8 *w*/%, d),e) and f): 15 *w*/%, g), h) and i): 50 *w*/%, j), k) and l): 70 *w*/%

of the Ni-Al layer surface, and areas with darker colors have pits.

The surface roughness of the Ni-Al layer samples was quantitatively analyzed using the AFM, and characterized by arithmetic-mean roughness (R_a) and root-mean-square roughness (*RMS*), that can be seen in **Table 3** for details that are consistent with the results obtained from the three-dimensional morphology of each sample. The variation range of Ni-Al layer roughness is relatively gentle when prepared by 8 *w*/% Al content in the cement.

Table 3: Roughness of Ni-Al layer fabricated with different Al content in the cement

Different aluminum contents	8 *w*/%	15 *w*/%	50 *w*/%	70 *w*/%
Arithmetic mean roughness R_a (nm)	5.13	98.3	2.28	12.5
Roughness per square meter *RMS* (nm)	7.18	122	2.98	30.8

J. J. Roa et al.[23] studied the friction, adhesion, and mechanical properties of single crystals, ceramics, and ceramic coatings by AFM, through the commonly used methods for analyzing and interpreting friction, adhesion, and nanoindentation data. E Rahimi et al.[24] researched the morphology modification mechanism of electrodeposited superhydrophobic nickel coating for enhanced corrosion performance and electrochemical measurements, the paper mainly pays attention to the surface topography of nickel films, which is characterized by the semi-contact mode of AFM. Thus, it can be seen that AFM can serve as a good auxiliary tool for detecting the morphology of materials, and through this method, more detailed and realistic morphological features can be obtained. This paper establishes a direct relationship between the layer composition and morphology through AFM, which was obtained from the surface information, providing a basis for subsequent friction and wear performance testing of the layer.

4 CONCLUSIONS

From the study, the following conclusions can be drawn:

(1) The metallographic photographs of the Ni-Al layer cross-section show that, when the Ni-Al layer thickness reaches a certain level, the diffusion resistance increases, thereby inhibiting further growth of the Ni-Al layer.

(2) The SEM analysis of the Ni-Al layer revealed that its morphology exhibits variations depending on the composition of the pack cement. EDS results demonstrated that the layer primarily consists of Fe and Al in varying proportions. Notably, the Ni element was absent on the surface of layers prepared with 50 *w*/% and 70 *w*/% Al, a phenomenon attributed to the depth of aluminum infiltration during the process.

(3) Two- and three-dimensional surface images through the atomic force microscopy (AFM) indicated that, the Ni-Al layer roughness changes relatively smoothly, which was prepared with 8 *w*/% Al content in the cement, the different roughness will lead to differences in friction and wear performance.

Acknowledgment

This research was funded by the Key R&D and Promotion Project of Henan Province in 2025 (No. 252102220078), the Key R&D and Promotion Special (Scientific Problem Tackling) Project of Henan Province (No. 212102210039), the Science and Technology Collaborative Innovation of Zhengzhou Project in 2022 and the High-level Introduction of Talent Research Start-up Fund of North China University of Water Resources and Electric Power (No. 4001/40680).

5 REFERENCES

[1] U. Gürol, Y. Altinay, A. Günen, Ö. S. Bölükbasi, M. Koçak, G. Çam, Effect of powder-pack aluminizing on microstructure and oxidation resistance of wire arc additively manufactured stainless steels, Surf. Coat. Tech.,468 (**2023**), 129742, doi:10.1016/j.surfcoat.2023.129742

[2] B. Rezaee, S. Rastegari, H. Eyvazjamadi, Formation mechanism of Pt-modified aluminide coating structure by out-of-the-pack aluminiz-

ing, Surf. Eng., 37 (**2021**), 343–350, doi:10.1080/02670844.2020.17412

[3] A. Heinzel, R. Fetzer, F. Lang, A. Weisenburger, S. Cataldo, F. Di Fonzo, G. Müller, Corrosion tests on austenitic samples with alumina and alumina-forming coatings in oxygen-containing stagnant Pb and turbulently flowing PbBi. J. Nucl. Mater.,596 (**2024**), 155121, doi:10.1016/j.jnucmat.2024.155121

[4] S. Sarraf, S. Rastegari, M. Soltanieh, Deposition of a low-activity type cobalt-modified aluminide coating by slurry aluminizing of a pre-Co-electroplated Ni-based superalloy (IN738LC). J. Mater. Res. Technol., 30 (**2024**): 1183–1193, doi:10.1016/j.jmrt.2024.03.132

[5] L. Yu, C. J. Xiao, W. Jiang, W. Li, S. Ni, M. Song, Effects of aluminizing on the microstructure and wear resistance of AISI 321 steel, Surf. Coat. Tech., 483 (**2024**), 130753, doi:10.1016/j.surfcoat.2024.130753

[6] X. Z. Fan, L. Zhu, W. Z. Huang, Investigation of NiAl intermetallic compound as bond coat for thermal barrier coatings on Mg alloy, J. Alloy. Compd., 729 (**2017**), 617–626, doi:10.1016/j.jallcom.2017.09.190

[7] X. Chen, C. Li, S. J. Xu, Y. Hu, G. C. Ji, H. T. Wang, Microstructure and microhardness of Ni/Al-TiB_2 composite coatings prepared by cold spraying combined with post annealing treatment, Coatings., 9 (**2019**) 9, 565, doi:10.3390/coatings9090565

[8] X. X. Zhao, X. M. Li, M. F. Li, C. G. Zhou, Comparison of the corrosion resistance of Ni_2Al_3 coating with and without Ni-Re interlayer in dry and wet CO_2 gas, Corros. Sci., 159 (**2019**) 10, 8121, doi:10.1016/j.corsci. 2019.108121

[9] Y. D. Wang, Y. P. Zhang, G. Liang, Q. L. Ding, Low temperature formation of aluminide coatings on the electrodeposited nanocrystalline Ni and its oxidation resistance with La_2O_3/CeO_2 nanoparticle dispersion, Vacuum., 173(**2020**), 109148, doi:10.1016/j.vacuum.2019.109148

[10] A. Bogdanov, V. Kulevich, V. Shmorgun, A. Taube, Formation of thermally grown aluminum oxide scale on the surface of Ni_2Al_3/Ni layered coating. Oxid. Met., 98 (**2022**), 199–216, doi:10.1007/s11085-022-10116-4

[11] K. M. Döleker, A. Erdogan, T. Yener, A. C. Karaoglanli, O. Uzun, M. S. Gök, S. Zeytin, Enhancing the wear and oxidation behaviors of the Inconel 718 by low temperature aluminizing, Surf. Coat. Tech., 412 (**2021**), 127069, dor:10.1016/j.surfcoat.2021.127069

[12] Y. Yürektürk, Effect of diffusion annealing on duplex coated pure titanium produced by hot-dip aluminizing and micro-arc oxidation, Surf. Coat. Tech., 433(**2022**), 128170, doi:10.1016/j.surfcoat.2022.128170

[13] Z. L. Zhan, Z. Liu, J. X. Liu, L. Li, Z. Li, P. B. Liao, Microstructure and high-temperature corrosion behaviors of aluminide coatings by low-temperature pack aluminizing process, Appl. Surf. Sci., 256 (**2010**), 3874–3879, doi:10.1016/j.apsusc.2010.01.043

[14] E. D. Varela, H. O. Abreu-Castillo, J. T. Pacheco, A. S. C. d'Oliveira, Pack-aluminizing mechanism in additively manufactured stainless steel, Surf. Coat. Tech.,, 496 (**2025**), 131651, doi:10.1016/j.surfcoat.2024.131651

[15] X. Wang, Y. Z. Fan, X. Zhao, A. Du, R. N. Ma, X. M. Cao, Process and high-temperature oxidation resistance of pack-aluminized layers on cast iron, Metals, 9(**2019**), 648, doi:10.3390/met9060648

[16] S. Majumdar, B. Paul, V. Kain, G. K. Dey, Formation of Al_2O_3/Fe-Al layers on SS 316 surface by pack aluminizing and heat treatment, Mater. Chem. Phys., 190 (**2017**), 31–37, doi:10.1016/j.matchemphys.2017.01.002

[17] L. Liu, C. Fan, H. Sun, F. Chen, J. Guo, T. Huang, Research progress of alumina-forming austenitic stainless steels: A review, Materials, 15 (**2022**): 3515, doi:10.3390/ma15103515

[18] J. Dong, Y. H. Sun, F. Y. He, H. T. Huang, J. P Zhen, Effects of substrate surface roughness and aluminizing agent composition on the aluminide coatings by low-temperature pack cementation, Mater. Res. Express, 6 (**2018**), 036409, doi:10.1088/2053-1591/aaf586

[19] J. Dong, Y. H. Sun, F. Y. He, Formation mechanism of multilayer aluminide coating on 316L stainless steel by low-temperature pack cementation, Surf. Coat. Tech., 375 (**2019**), 833–838, doi:10.1016/j.surfcoat.2019. 08.005

[20] N. N. Li, L. Xu, L. Huang, Y. P. Tong, Z. Q. Jiang, K. L. Li, Preparation and hardness of a functionally graded Ni-Al coating, Mater. Tehnol., 57 (**2023**) 1, 27–33, doi:10.17222/mit.2022. 650

[21] Z. D. Xiang, P. K. Datta, Formation of nickel aluminide/nickel hybrid coatings on alloy steels by two step process of nickel plating and low temperature pack aluminisation, Materi. Sci. Tech-lond, 25 (**2009**), 733–738, doi:10.1179/174328407X245

[22] D. Bogdan, I. G. Grosu, C. Filip, How thick, uniform and smooth are the polydopamine coating layers obtained under different oxidation conditions An in-depth AFM study. Appl. Surf. Sci., 597 (**2022**), 153680, doi:10.1016/j.apsusc.2022.153680

[23] J. J. Roa, G. Oncins, J. Díaz, X. G. Capdevila, F. Sanz, M. Segarra. Study of the friction, adhesion and mechanical properties of single crystals, ceramics and ceramic coatings by AFM, J. Eur. Ceram. Soc., 31 (**2011**), 429–449, doi:10.1016/j.jeurceramsoc.2010.10.023

[24] E. Rahimi, A. Rafsanjani-Abbasi, A. Kiani-Rashid, H. Jafari, A. Davoodi. Morphology modification mechanism of electrodeposited superhydrophobic nickel coating for enhanced corrosion performance studied by AFM, SEM-EDS, and electrochemical measurements, Colloid. Surface. A., 547 (**2018**), 81–94, doi:10.1016/j.colsurfa.2018.03.045